# Online Process Control of a Pharmaceutical Intermediate in a Fluidized-Bed Drier Environment Using Near-Infrared Spectroscopy

**ARTICLE** *in* ANALYTICAL CHEMISTRY · MAY 2010

Impact Factor: 5.64 · DOI: 10.1021/ac1004579 · Source: PubMed



**5 AUTHORS**, INCLUDING:

Julia Märk
Technische Universität Berlin
**16** PUBLICATIONS **135** CITATIONS
SEE PROFILE

Christian Huck
University of Innsbruck
**268** PUBLICATIONS **3,349** CITATIONS
SEE PROFILE

*Anal. Chem.* **2010,** *82,* 4209–4215

# Online Process Control of a Pharmaceutical Intermediate in a Fluidized-Bed Drier Environment Using Near-Infrared Spectroscopy

**Julia Märk,[†,‡] Martin Karner,[‡] Max Andre,[‡] Jochen Rueland,[‡] and Christian W. Huck*[,†]**

*Institute of Analytical Chemistry and Radiochemistry, Leopold-Franzens University, Innrain 52a, 6020 Innsbruck, Austria, and Sandoz GmbH, Biochemiestrasse 10, 6250 Kundl, Austria*

**In the production plant of an antibiotic substance, a new fluidized-bed drier has been installed. For online process control of the drying progress and determination of the ideal drying end point, a continuous near-infrared spectroscopic (NIRS) measuring setup was implemented to rapidly and simultaneously gain all essential product information. A bypass system outside the drier combined with a robust process probe proved to provide the best sampling system geometry. The spectrometer was equipped with an additional laboratory probe for complementary offline analysis. Multivariate calibrations for product assay, water content, and residual solvent were calculated, optimized, and compared for the two probes. The final root-mean-square error of cross validation (RMSECV) for the process probe could be reduced to 0.81% for the product assay, 0.25% for water, and 0.06% for acetone. The laboratory-probe prediction values show good agreement with reference data during the testing period. The calibrations of the process probe were checked by comparing its predictions to those of the validated laboratory probe. The monitoring system could be automated to a large extent, and product quality could be improved considerably. The established technology is of high importance for the pharmaceutical industry carrying out high-throughput routine analysis because of its advantages in terms of of time and cost reductions.**

Strong compulsory regimentation and economic pressure require the development and implementation of suitable new techniques for process control and analysis in the pharmaceutical industry.[1,2] For improved drug security in complicated manufacturing procedures, interest in complete quality control is rising in an effort to avoid rework processes. The extensive analysis of all deployed materials, intermediates, and products leads to a higher degree of process stability and can contribute to a faster compensation for deviations,[3] especially at critical production steps. Conventionally, wet chemical analysis was applied to gather the required information—at high chemical, financial, and time expense. Therefore, such analyses are increasingly being replaced by efficient spectroscopic methods.

Near-infrared spectroscopy (NIRS) has become a popular process control tool with a broad range of applications for precise material characterization. This fast and noninvasive technique reveals a high content of information by exciting overtone and combination vibrations in the irradiated substance, allowing for the assessment of physical and chemical sample characteristics at the same time.[4−7] Multivariate data evaluation methods[8,9] can be used to investigate the relation of spectral data from different wavelength regions in one context to extract the highest degree of information.[10] With an appropriate sampling system, the sample compositions can be determined nondestructively directly in the production area during manufacturing[11−16] with various in-, at-, or online configurations.[17,18] The diverse applications so far cover

* Corresponding author: Prof. Dr. Christian Huck, Head of Spectroscopy Group Institute of Analytical Chemistry and Radiochemistry, Innrain 52a, 6020 Innsbruck, Austria. Tel.: +43 512 507 5195. Fax: +43 512 507 2965. E-mail: Christian.W.Huck@uibk.ac.at.

† Leopold-Franzens University.

‡ Sandoz GmbH.

(1) Lopes, J. A.; Costa, P. F.; Alves, T. P.; Menezes, J. C. *Chemom. Intell. Lab. Syst.* **2004**, *74* (2), 269–275.

(2) Ribeiro, M. P. A.; Padua, T. F.; Leite, O. D.; Giordano, R. L. C.; Giordano, R. C. *Chemom. Intell. Lab. Syst.* **2008**, *90* (2), 169–177.

(3) *Guidance for Industry: PAT—A Framework for Innovative Pharmaceutical Development, Manufacturing and Quality Assurance*; U.S. Food and Drug Administration, U.S. Department of Health and Human Services: Washington, DC, Sep 2004; http://www.fda.gov/downloads/Drugs/GuidanceComplianceRegulatoryInformation/Guidances/UCM070305.pdf.

(4) Heigl, N.; Petter, C. H.; Najam-Ul-Haq, M.; Rainer, M.; Vallant, R. M.; Bonn, G. K.; Huck, C. W. *J. Near Infrared Spectrosc.* **2008**, *16* (3), 211–221.

(5) Heigl, N.; Petter, C. H.; Rainer, M.; Najam-ul-Haq, M.; Vallant, R. M.; Bakry, R.; Bonn, G. K.; Huck, C. W. *J. Near Infrared Spectrosc.* **2007**, *15* (5), 269–282.

(6) Olinger, J. M.; Griffiths, P. R. *Anal. Chem.* **1988**, *60* (21), 2427–2435.

(7) Otsuka, M. *Powder Technology* **2004**, *141* (3), 244–250.

(8) Eriksson, L.; Johansson, E.; Kettaneh-Wold, N.; Trygg, J.; Wikström, C.; Wold, S. *Multi- and Megavariate Data Analysis. Part I: Basic Principles and Applications*; Umetrics Academy: Umeå, Sweden, 2006.

(9) Kessler, W. *Multivariate Datenanalyse für die Pharma-, Bio- und Prozessanalytik*; Wiley-VCH: Weinheim, Germany, 2007.

(10) Wold, S.; Trygg, J.; Berglund, A.; Antti, H. *Chemom. Intell. Lab. Syst.* **2001**, *58* (2), 131–150.

(11) Mattes, R.; Schroeder, R.; Dhopeshwarkar, V.; Kowal, R.; Randolph, W. Pharm. Tech. 2004.

(12) Namkung, H.; Lee, Y.; Chung, H. *Anal. Chim. Acta* **2008**, *606* (1), 50–56.

(13) Norris, T.; Aldridge, P. K.; Sekulic, S. S. *Analyst* **1997**, *122*, 549–552.

(14) Rantanen, J.; Räsänen, E.; Antikainen, O.; Mannermaa, J. P.; Yliruusi, J. *Chemom. Intell. Lab. Syst.* **2001**, *56* (1), 51–58.

(15) Watari, M.; Higashiyama, H.; Mitsui, N.; Tomo, M.; Ozaki, Y. *Appl. Spectrosc.* **2004**, *58* (2), 248–255.

(16) Zachariassen, C. B.; Larsen, J.; van den Berg, F.; Engelsen, S. B. *Chemom. Intell. Lab. Syst.* **2005**, *76* (2), 149–161.

(17) Clark, D.; Pysik, A.; Pivonka, D. E.; Chalmers, J. M.; Griffiths, P. R. In *Applications of Vibrational Spectroscopy in Pharmaceutical Research and Development*; John Wiley & Sons: New York, 2007.

(18) Mark, H.; Workman, *J. Anal. Chem.* **1986**, *58* (7), 1454–1459.

10.1021/ac1004579 
Published on Web 04/20/2010

the primary production of pharmaceutical substances (reaction monitoring of crystallization and distillation processes and identification of polymorph forms) as well as secondary production (final drug machining including milling, granulation, drying, blending, compression, and coating).[19−24]

With online NIR control systems of drying steps, real-time product information can be used to reduce the risk of overdrying and to improve product yield and quality at higher cycle times. Minimized manual sampling decreases safety concerns, and considerably less reference analysis limits environmental impacts and saves money.[25] These advantages have already been utilized in the implementation of NIR moisture content evaluation systems in fluidized-bed granulation steps[26,27] and in a continuous conversion reactor.[28] Several successful industrial applications of NIR spectroscopy for the monitoring of different dryer types and geometries with comparably long cycle times have also been reported.[29,30]

In this study, an automated online monitoring system based on the continuous evaluation of NIR spectroscopic data was developed for a fluidized-bed drying process of a pharmaceutical intermediate. The objective of the study was to determine the ideal end point to stop the drying course and therefore attain the best product assay at sufficiently reduced levels of water and solvent content at the same time. The NIR device continuously collects spectral data during the whole drying process and performs automated evaluation to effectively follow and assess the drying progress on the basis of the calculated product, assay, and water contents supplemented with the fluidized-bed temperature profile.

## EXPERIMENTAL SECTION

**Instrumentation.** A SOLVIAS REFLECTOR process probe (PP; Solvias, Basel, Switzerland) combined with a Fourier-transform NIR spectrometer (Matrix-F, Bruker Optik GmbH, Ettlingen, Germany) that meets the required automation criteria is used for the control system implementation. The spectrometer covers the wavelength range from 4000−12000 $cm^{-1}$ with a variable resolution down to 1 $cm^{-1}$. The probe made of stainless steel offers temperature stability up to 130 °C with an immersion depth of 300 mm and a 12-mm tip diameter. The 3-mm beam spot is directed onto the sample substance through a sapphire window. The probe placed in the production area (EX zone 22) is connected to the spectrometer device in the analysis room via coupled 2- and 5-m fiber optic cables. The spectrometer device is additionally equipped with a laboratory probe (LP) using a multiplexer connection to enable complementary offline spectra recording. These spectra were recorded using a probe fixture and a sample hoist. Resolution was set to a standard value of 8 $cm^{-1}$ with the number of scans set to 24, corresponding to a 15-s expenditure of time to compromise between prediction precision and temporal effort to archive enough data points to effectively follow the drying process.

**Automation and Software.** The automatic trigger for continuous measurements is given by the process control system via a PROFIBUS interface using an OPC client/server system on the control PC running the OPUS 6.5 PROCESS package (Bruker). Data evaluation is performed immediately with the OPUS/QUANT module according to the respective calibrations. The resulting values are sent back to the process control system and displayed on the switch-room monitoring screen. The spectra are labeled according to their measuring point in time and archived in a network folder.

**Reference Methods.** *Water.* To quantify the water content of the samples, a Karl Fischer back-titration method was performed using a Mettler-Toledo DL 39 Coulometer device together with a Stromboli sample changer oven (Mettler-Toledo GmbH, Greifensee, Schweiz). Temperature was set at 110 °C. The sample was weighed to 0.3−0.6 g and swept with a molecular-sieve-dried air stream for approximately 8 min.

*HPLC.* Product assay was determined by isocratic high-performance liquid chromatography (HPLC). A YMC-Pack C18 RS (150 mm, 4.6 mm i.d., S-5 $\mu$m) column together with an Agilent 1090 series instrument (Agilent Technologies, Palo Alto, CA) was applied for separation of a weighed, dissolved sample of 20 mg. UV detection was accomplished at 260 nm.

*GC.* The respective content of acetone was analyzed by gas chromatography using an Agilent 6890 system with a Gerstel MPS2 (GERSTEL GmbH & Co. KG, Mülheim, Germany) injection method. Approximately 200 mg of sample was weighed, dissolved, and sealed for a 1 mL headspace injection. An HP-1 stationary phase (dimethylpolysiloxane phase, 30 m, 250 $\mu$m i.d., 1 $\mu$m) was applied for separation, combined with a flame ionization detector at 250 °C.

HPLC and GC programming and data evaluation were performed with Chromeleon V67 (Dionex Corporation, Sunnyvale, CA).

## RESULTS AND DISCUSSION

In the production plant of an antibiotic intermediate, a new fluidized-bed drier was installed to complement the former slow vacuum paddle drying method that leads to limited product quality, subjecting the pharmaceutical product to mechanical stress and long-term direct heat impact. The main objectives were capacity improvement and product composition optimization, which is critical for further machining. The hot gas stream serves as a heat source and conducts the solvent vapor from the area of contact.[31] Dwell time and filling quantity (200-kg batch load) are considerably lower than for the paddle drying process.[32] With preferably


(19) Lai, X.; Zheng, Y.; Sondergaard, I.; Josephsen, H.; Lowenstein, H.; Larsen, J. N.; Ipsen, H.; Jacobsen, S. *Vaccine* **2007**, *25* (52), 8732–8740.
(20) Li, W.; Johnson, M. C.; Bruce, R.; Rasmussen, H.; Worosila, G. D. *Pharm. Biomed. Anal.* **2007**, *43* (2), 711–717.
(21) Luypaerta, J.; Massart, D. L.; Vander Heyden, Y. *Talanta* **2007**, *72* (3), 865–883.
(22) Sarraguca, M. C.; Lopes, J. A. *Vib. Spectrosc.* **2009**, *49* (2), 204–210.
(23) Sekulic, S. S.; Ward, H. W.; Brannegan, D. R.; Stanley, E. D.; Evans, C. L.; Sciavolino, S. T.; Hailey, P. A.; Aldridge, P. K. *Anal. Chem.* **1996**, *68* (3), 509–513.
(24) Ufret, C.; Morris, K. *Drug Dev. Ind. Pharm.* **2001**, *27*, 719–729.
(25) Bakeev, K. A. *Spectroscopy* **2004**, *19* (1), 39–42.
(26) Frake, P.; Greenhalgh, D.; Grierson, S. M.; Hempenstall, J. M.; Rudd, D. R. *Int. J. Pharm.* **1997**, *151* (1), 75–80.
(27) Rantanen, J.; Antikainen, O.; Mannermaa, J. P.; Yliruusi, J. *Pharm. Dev. Technol.* **2000**, *5* (2), 209–217.
(28) Ward, H. W.; Sistare, F. E. *Anal. Chim. Acta* **2007**, *595* (1−2), 319–322.
(29) Burgbacher, J.; Wiss, J. *Org. Process Res. Dev.* **2008**, *12*, 235–242.
(30) Wildfong, P. L. D.; Samy, A. S.; Corfa, J.; Peck, G. E.; Morris, K. R. *J. Pharm. Sci.* **2002**, *91* (3), 631–639.
(31) Chulia, D.; Deleuil, M.; Pourcelot, Y. In *Powder Technology and Pharmaceutical Processes*; Elsevier: New York, 1994.
(32) Masuda, H.; Higashitani, K.; Yoshida, H. In *Powder Technology Handbook*; Taylor & Francis Group: Oxford, U.K., 2006.

**Scheme 1. Key Parameters of the Fluidized-Bed Drying Process Related to the Mass of the Moist and Dried Products**

| | Moist product | | Dry product |
|---|---|---|---|
| Assay % | 60 - 67 | | ≥ 88 |
| Water % | 8 - 10 | $N_2$-circuit | ≤ 2 |
| Acetone % | 25 - 30 | | ≤ 1 |

short exposure to gas temperatures of at most 130 °C, the powder is dried gently and efficiently, with final assay values exceeding 90%. Monitoring and control of a fluidized-bed drying process according to the temperature characteristics only—as conducted for the paddle drier—might not be sufficiently accurate because of high product density variations and fast drying progression.

**Expected Drying Devolution.** The wet product is transferred from the preceding production step into a bunker from which the fluidized-bed drier is loaded batchwise. The rough product composition was previously determined in a small-scale pilot study using a miniaturized version of the drying system to estimate the expected proceedings. The whole process lasts for 10−15 min, with the ideal end point reached at the maximum product assay with the lowest possible water content, where thermal product degradation does not yet occur. The obtained key process parameters are presented in Scheme 1. The majority of the solvent evaporates immediately, and subsequent equilibration is reached in the hot gas stream, limiting minimum residual solvent to around 1%. The dry pharmaceutical is discharged through an outlet valve with hot nitrogen gas, where considerable further drying can occur. Such effects have to be taken into account when determining the proper drying end point to minimize this loss factor.

**Sampling System.** In the first step, a suitable measuring setup had to be selected. Measuring configurations directly inside the drier, such as with a contact-free measurement head applied through a window[33] or an integrated probe positioned toward the product stream,[11] were discarded. Lack of spectral reproducibility at high density and temperature variations in the product might impede the achievement of the desired accuracy,[34] and sampling difficulties for reference analysis could occur. A model-free calibration using spectral changes that can be used for the determination of product homogeneity at mixing steps[23] is not convenient in this case. For the complicated multicomponent pharmaceutical with partly correlating components, the required specificity might not be reached. To minimize all of these factors of uncertainty, a bypass configuration was designed to record spectra outside the drier. The bypass system (Figure 1) had to meet the following requirements: a fast and reliable filling and purging procedure, a reproducible and defined sample density during the measurements, an efficient probe tip cleaning mechanism to avoid artifacts, and both optical and easy mechanical access to the sample material for operational control and reference analysis. As long as the powder does not scratch the probe window or produce irreversible deposits, precisions comparable to laboratory measurements can be reached.[35] The interior of the bypass should be kept simple and the sample volume should be kept small to reduce temporal effort for each measuring cycle. The final system was made of glass with the probe tip pointing outward to enable direct visual access to inspect proper coverage of the probe. With a vacuum pump, moist product is withdrawn from the drier until the bypass is sufficiently loaded. After the recording of the spectra the whole sample powder is blown back with nitrogen gas. The probe is cleaned with a directed gas stream from across to avoid contamination. The pumping power has to be adjusted to the respective dimensions of the bypass volume and tubing. Especially toward the end of a run, high pump rotation speed is needed to prevent partially insufficient bypass inflation, as the bulk material is then predominantly located in the upper part of the drier. Sample drawing is conducted manually with a spatula through a sealed window on the side of the bypass. The measurement course was optimized after implementation by setting the start signal at a minimum temperature of 85 °C with the maximum yield range still well established. In this way, sample deposits of wet product and condensation effects are minimized.

**Calibration Procedure.** Calibrations had to be calculated for both probes for product assay, water, and acetone contents. During the calibration stage, lasting for several weeks, drying conditions were systematically changed with respect to filling capacity and operating temperature. Therefore, the calibrations can account for high variability of these parameters, and a broad product quality range can be captured. To expand the calibration range, spectral data of both the still-moist pharmaceutical and almost-burned material would be preferable. As this does not compromise with economic considerations, only a few batches in the adjustment period met these conditions.

The attenuation of hydrogen bonding due to higher temperatures results in a band shift toward higher frequencies.[36,37] Therefore, this parameter should be stabilized or incorporated in the calibration by systematic variation. However, the effect of temperature on hydrogen bonding is far less influential for the calibration of powdery substances than it is for liquid samples.[38] The bulk set of process-probe calibration spectra was recorded systematically at drier internal temperatures of 90, 100, and 105 °C and at the drying end point at approximately 110 °C. Each spectrum was automatically assigned a unique name including the exact timestamp of recording to enable proper matching of the reference analysis results. Figure 2 displays a typical set of changing spectra of the increasingly dry material during a drying course used for calibration. The spectra of the intermediate show a high fiber-optic-related noise level at wavenumbers below 4200 $cm^{-1}$ and low intensities in the higher-wavenumber region. Therefore, only the domain between 4200 and 9000 $cm^{-1}$ was considered for multivariate calibration. The basic spectral feature of the complex antibiotic molecule containing a $\beta$-lactam structure is the massive water peak at 5206 $cm^{-1}$ strongly varying in size. A second broad peak originating from water vibrations dominates the wavenumber range around 7000 $cm^{-1}$.


(33) Moes, J. J.; Ruijken, M. M.; Gout, E.; Frijlink, H. W.; Ugwoke, M. I. *Int. J. Pharm.* **2008**, *357* (1−2), 108–118.

(34) Benedetti, C.; Abatzoglou, N.; Simard, J. S.; Mc Dermott, L.; Léonard, G.; Cartilie, L. *Int. J. Pharm.* **2007**, *336* (2), 292–301.

(35) Kemeny, G. J. In *Handbook of Near-Infrared Analysis*, 2nd ed.; Burns, D. A., Ciurczak, E. W., Eds.; CRC Press: Boca Raton, FL, 2001; pp729−782.

(36) Workman, J. In *Near Infrared Spectroscopy: The Future Waves*; Davies, A. M. C., Williams, P., Eds.; NIR Publications: Chichester, U.K., 1996; pp 6−13.

(37) Togersen, G.; Arnesen, J. F.; Nilsen, B. N.; Hildrum, K. I. *Meat Sci.* **2003**, *63*, 515–523.

(38) Osborne, B. G.; Fearn, T.; Hindle, P. H. *Practical NIR Spectroscopy*, 2nd ed.; Longman Scientific & Technical: Essex, U.K., 1993.

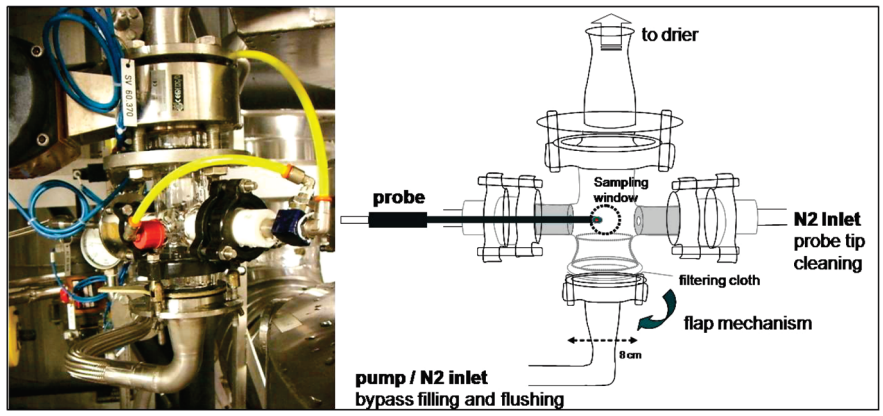


**Figure 1.** (Left) Final implementation of the sampling system in the production area (right) and schematic view of the bypass configuration.

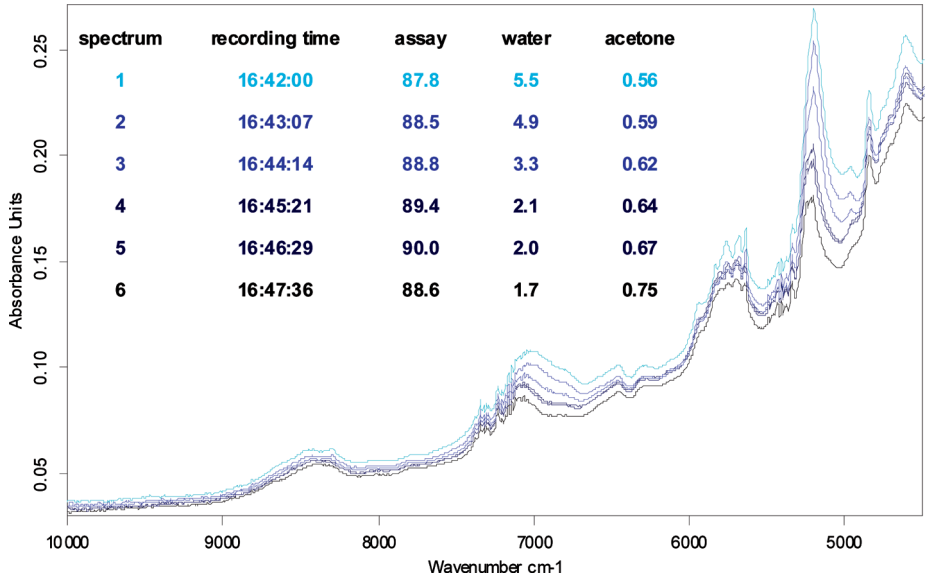


**Figure 2.** Examples of the last six spectra recorded just before reaching the drying end point with the respective time stamps and reference values in percentages.

In addition to these obvious spectral shifts, the rapidly changing product composition, which is specified in the figure by the respective reference values, can be easily recognized in a broad range of the whole NIR region. Signal features in the range of 5600−5900 $cm^{-1}$ arise from CH and $CH_2$ first overtone vibrations. The spectral characteristics around 4100−4400 $cm^{-1}$ refer to CH combination bands of fundamental vibrations and deformation modes.[39] They reveal complex spectral features at high absorbance values. Patterns in the region of 7000−7400 $cm^{-1}$ arise from CH combination bands of overtone and fundamental vibrations. For example, the narrow band at 7184 $cm^{-1}$ is generated from a combination vibration of 2 × CH stretch and CH bending of the $CH_2$ group. Additionally, the small peak at 4972 $cm^{-1}$ could possibly be assigned to a combination band of the fundamental NH stretch with the amide II vibration.

Immediately after spectral recording inside the bypass, sample material was skimmed into a glass vial, tempered at room temperature, and additionally measured with the laboratory probe two to three times at intermediate probe tip relocation. Subsequently, the substances were characterized by the respective reference methods. For the calibration of the laboratory probe, mostly the same samples were utilized to keep reference analysis efforts to a minor level. As spectral recording can be performed at ever-repeatable, exactly defined conditions, the calibration of the laboratory probe proved to be much easier and faster. For practical reasons, as results are at immediate disposal, the laboratory-probe measurement could partly serve as a reference analysis method for process-probe calibration after an adequate standard validation procedure.

*Process Probe.* The process-probe calibration set was expanded with a set of spectra recorded offline, outside the bypass in separate glass vials to broaden the temperature range and integrate sufficient bulk density variations. According to these tactics, a higher precision using uniform recording conditions is balanced by a considerable enhancement in calibration robustness. Temperature variations inside the bypass can distort the calibrations as a result of potential correlations to the product parameters to be determined. To test this approach, prediction values of externally recorded spectra with a calibration consisting only of bypass spectra measured online as well as predictions of bypass

(39) Weyer, L. G.; Lo, S. C. In *Handbook of Vibrational Spectroscopy*; Chamers, J. M., Griffiths, P. R., Eds.; John Wiley & Sons: Chichester, U.K., 2002; Vol. 3, pp 1817−1837.

**Table 1. Details of the Calibrations Obtained for the Three Different Parameters for the Two Probe Types[a]**

| | product | | water | | acetone | |
|---|---|---|---|---|---|---|
| | LP | PP | LP | PP | LP | PP |
| calibration spectra | 119 | 167 | 114 | 153 | 157 | 33 |
| range (%) | 68.6−93.0 | 84.7−93.0 | 0.30−8.20 | 0.39−7.15 | 0.20−4.40 | 0.30−0.93 |
| rank | 5 | 7 | 3 | 7 | 7 | 4 |
| $R^2$ | 96.1 | 81.6 | 98.2 | 93.4 | 96.1 | 77.4 |
| RMSECV | 0.71 | 0.81 | 0.20 | 0.25 | 0.11 | 0.06 |
| pretreatments | derivative 1 + MSC | derivative 2 | derivative 1 + SNV | derivative 1 | derivative 1 + MSC | derivative 1 + SLS |
| wavenumber regions ($cm^{-1}$) | 8914−6098<br>4602−4247 | 7502−5446 | 8817−5446 | 7502−6098 | 8736−7498<br>6102−5446 | 6102−5446 |

[a] Abbreviations: LP, laboratory probe; PP, process probe; RMSECV, root-mean-square error of cross validation; MSC, multiplicative scatter correction; SNV, standard normal variate correction; SLS, straight line subtraction.

spectra with a calibration composed of only offline spectra were investigated. In both cases, predictions showed slight systematic deviations from their reference values. Combining the two classes of spectra results in a minor decrease of precision of the calibration of product assay but higher prediction stability, which is preferable because of limited control prospects inside the bypass system. The calibration of the water content with online and offline spectra even shows a higher accuracy and better prediction values, as this parameter is highly sensitive to temperature variations.[40,41] As high acetone content induces variances and troubles within the further production steps, this parameter was additionally integrated in the monitoring of the drying process for purely informative reasons. The majority of the acetone content evaporates already before the first bypass filling, and therefore, only a spectra set with a narrow bandwidth of reference values is available for calibration.

*Laboratory Probe.* To retain sufficient data points in the critical dry region, several overdried batches originating from pilot test runs of the drier were measured and incorporated into the laboratory-probe calibration set. To ensure that these slightly burned batches with product assays far below 80% did not distort the calibration due to modified powder texture, their prediction values were tested for correctness with former NIR methods prior to integration of the spectra. Few paddle drier material spectra were additionally incorporated into these calibrations to extend their applicability to product material arising from both drying methods. The range of all calibration parameters is therefore much more diversified for the laboratory-probe calibration.

**Calibration Results.** The spectra set composition was optimized, omitting low-quality spectra due to inconsistent bypass fillings and maximizing the chemical bandwidth. All calibration spectra were subsequently mean-centered and subjected to a range of standard spectral pretreatment methods such as vector normalization, multiplicative scatter correction, first and second differentiation, and different combinations thereof. In addition, the consulted spectral regions were varied to choose the wavenumbers containing the required information, which therefore are most suitable for calibration. The final pretreatment methods were chosen for each model by their prediction power in a conventional approach.[9,42−44] Various calibrations were tested by estimating their leave-one-out root-mean-square error of cross validation (RMSECV), as well as their prediction error (RMSEP) for a specified test set of samples excluded from calibration

$$\mathrm{RMSEP/RMSECV} = \sqrt{\frac{\sum_{i=1}^{N} (y_{\mathrm{ref}\_i} - y_i)^2}{M}} \qquad (1)$$

where $y_{\mathrm{ref}\_i}$ corresponds to the parameter value determined by reference methods and $y_i$ corresponds to the NIR prediction of the test set sample and the cross-validation sample, respectively. $M$ represents the number of samples in the test/calibration set.

Finally, the pretreatment methods and wavenumber ranges resulting in the lowest calibration errors giving a good correlation of the NIR predictions and reference values were applied before further model optimization. The number of principal components was set at the minimum prediction error. A summary of all characteristic parameters of the elaborated calibrations is presented in Table 1. The cited error of cross validation could be mainly reduced to the error of the respective reference methods, confirming the applicability of the NIR monitoring setup. For both parameters, water and assay, the coefficients of determination ($R^2$ values) are closer to 1 with minor error values for the laboratory-probe calibrations compared to those of the process probe at a lower number of principal components. This is caused by the broad calibration range and the higher quality of the laboratory spectra. The exclusion of the main water peak signal at 5000 $cm^{-1}$ because of the fact that its strong temperature dependence causes nonlinear effects[45,46] induces more precise calibration results. The error of water prediction is comparable to those of similarly configured NIR online applications.[1,47]

**Testing of the Methods.** The calibrations were tested for their reliability over an extensive period with independent test samples. To check the laboratory-probe calibrations, numerous elected production batches were investigated with NIRS and the respective reference methods in parallel for several months. In Figure 3, comparisons between those differently determined fractions of


(40) Czarnecki, M.; Ozaki, Y. *Phys. Chem. Chem. Phys.* **1999**, (1), 797–800.
(41) Watari, M.; Ozaki, Y. *Appl. Spectrosc.* **2005**, *59* (5), 600–610.
(42) Adams, M. J. *Chemometrics in Analytical Spectroscopy*; RSC Analytical Spectroscopy Monographs; Royal Society of Chemistry: London, 1995.
(43) Kramer, R. *Chemometric Techniques for Quantitative Analysis*; Marcel Dekker: New York, 1998.
(44) Mark, H. *Principles and Practice of Spectroscopic Calibration*; John Wiley & Sons: New York, 1991.
(45) Cozzolino, D.; Liu, L.; Cynkar, W. U.; Dambergs, R. G.; Janik, L.; Gishen, M. *Anal. Chim. Acta* **2009**, *588* (2), 224–230.
(46) Peinado, A. C.; van den Berg, F.; Blanco, M.; Bro, R. *Chemom. Intell. Lab. Syst.* **2006**, *83* (1), 75–82.
(47) Mattes, R.; Root, D. E.; Birkmire, A. P. *Spectroscopy* **2005**, *20*, 14–17.

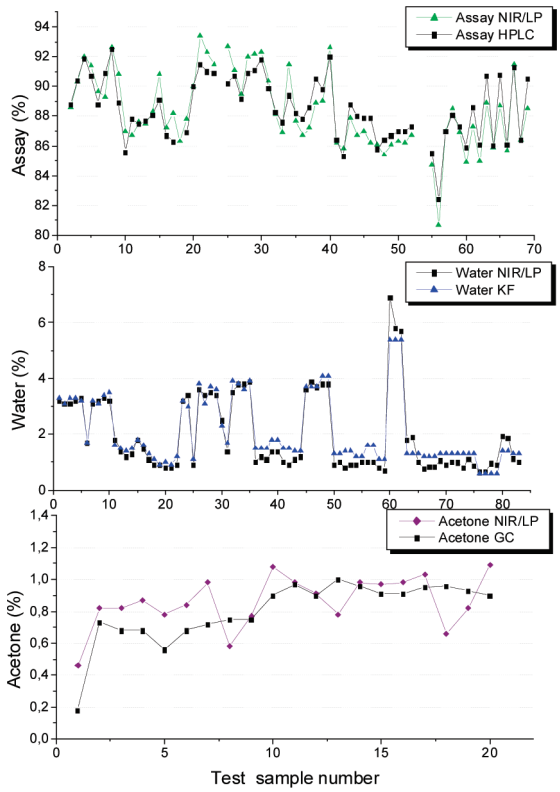


**Figure 3.** Comparison of the NIR prediction values determined using the laboratory probe with the reference values for product assay, water, and acetone.

assay, water, and acetone contents of those samples are presented in chronological order. All parameters can be well predicted with the NIR methods, and there are no major deviations within the reviewed time period. All batches with water values above 2% were fabricated with the paddle drier procedure; low water contents refer to the new fluidized-bed drying step. The average deviations of the NIR predictions from the reference values for all disposable samples are 0.87% for assay (64 samples, maximum difference 2.5%), 0.28% for water (83 samples, maximum difference 1.5%), and 0.14% for acetone (20 samples, maximum difference 0.3%), which all lie within the range comparable to the error of cross validation of the calibration sets.

*Probe Alignment.* The process-probe calibrations of assay and water contents were tested according the comparison of their prediction values with those of the laboratory probe, which was approved as the validated reference method. The test batch set, as displayed in Figure 4, covers a broad time period starting from the drier validation and NIR control system implementation and two check-up campaigns several months later. Most notably, water prediction values show good agreement in both cases. Assay content values appear to deviate systematically, especially for low-content samples, but feature a synchronous devolution to the laboratory-probe predictions by trend. This deficiency is due to the lack of sufficient calibration spectra in the low-content region, as flexibility in the production environment is restricted. For 64 investigated samples, the average discrepancy in process- and laboratory-probe predictions is 1.2% for product assay and 0.6% for water. The higher accuracy of the determined water content

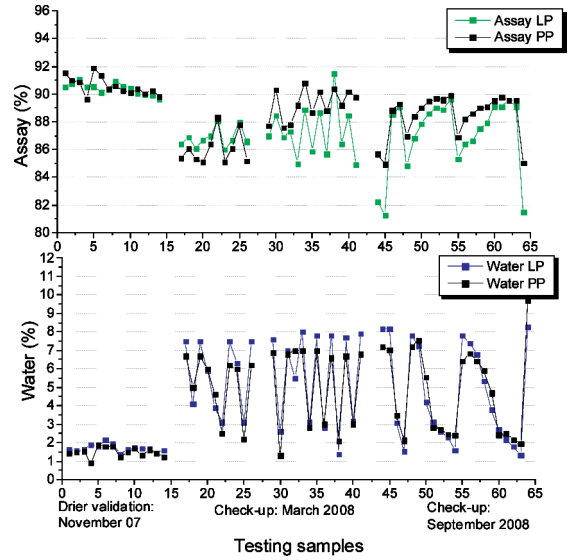


**Figure 4.** Comparison of the NIR prediction values of the laboratory and process probes.

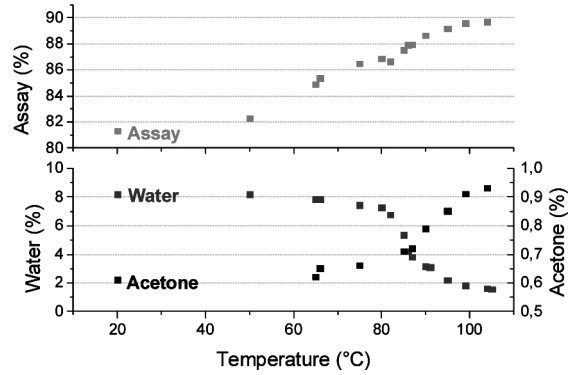


**Figure 5.** Chronological, temperature-dependent evolution of the product composition with respect to product assay, water, and acetone contents.

has to be taken into account in the control of the drier operation mode. Therefore, water was chosen to be the crucial monitoring parameter.

**Routine Application.** *Drier Validation with NIRS.* Both the offline NIR control system and the online monitoring setup proved to be of great value for the validation of the new drying process. Product substance had to be analyzed at all stages of the drying process to ensure the unobjectionable operation of the dryer and the applicability of the new drying approach to the chosen pharmaceutical. With laboratory-probe measurement, several complete batches, each consisting of 14 drying runs, could be tested instantaneously for their composition as moist product, during the drying run and in the final packaging stage at marginal effort. Product homogeneity and repeatability of the NIR predictions were proved and subbatch mixing times could be efficiently optimized to the required minimum. The stability and conformity of each drying run could be investigated using the bypass spectra predictions. Using NIR monitoring, product quality could be improved at each drying course.

Figure 5 shows a detailed charted example of the product composition as a function of the drier interior temperature determined with the NIR bypass measurement. Although the product assay increases linearly with temperature, the water

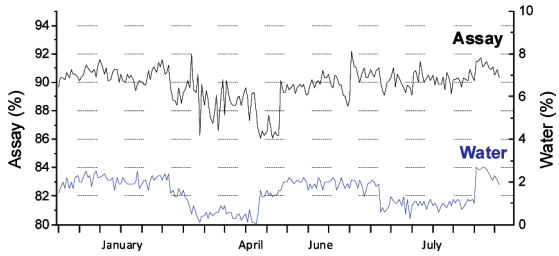


**Figure 6.** Development of the end product composition determined with online NIR measurements over several months.

content is strongly reduced at 80 °C. The relative percentage content of acetone rises during the incremental drying progress, as water is steadily evaporated.

*Drying Process Control.* The temporal gap between each subsequent spectral recording initiated with the first bypass filling at the stated minimum temperature is slightly more than 1 min. On average, six NIR spectra are evaluated for each routine drying course. This permits the efficient and accurate monitoring of the critical end phase of the process. Different modes of drying operation result in various combinations of water and product content. The values for water are in the range of 0−2%, and assay balances are between 86 and 92% at high variability, which can be inferred from the data presented in Figure 6. The results for each drying end-point spectrum evaluation are given for the observation period of several months.

## CONCLUSIONS

The surveillance of the fluidized-bed drier with NIRS permits an efficient control of the drying process and offers the possibility for its constant adaptation and improvement. Especially within the first optimization period of the drier operation mode, the spectroscopic monitoring system proved to be of great value. Routine operation is now performed by combining the NIR results with the drying temperature progression. Any deviation from the normal drying course can be detected easily and instantaneously. The product quality has been improved and stabilized, and the low water content allows for reduced chemical expenses during further production steps. The large amount of available information facilitates the evaluation and interpretation of process data. The additional offline measurement could be well established because of its flexibility and broad application range at low costs and could to a high gain in both process and product knowledge using statistical evaluation methods. Experiments on the influence of different physical and chemical parameters on the product could be investigated at no effort.

Nevertheless, the system has to be tested regularly to ensure flawless operation. To ensure accuracy and reliability of the methods, every 10th batch is additionally investigated with reference techniques by default. Therefore, drifts and deviations arising from changes in the material or the manufacturing procedure, which could influence the product matrix and lead to wrong prediction values can be detected immediately. As soon as any changes in the preceding production steps occur, recalibration and the incorporation of new samples are mandatory. The system proved to work very stably; however, an update was performed after approximately six months of operation to broaden the range of the calibrations for water and to further reduce the calibration error for assays.

## ACKNOWLEDGMENT

We thank Dr. Renate Dietl (Bruker Optics) for her help and extended discussions on the phone. Moreover, the authors acknowledge Leopold-Franzens University (Innsbruck, Austria) for financial support.

Received for review February 19, 2010. Accepted April 6, 2010.

AC1004579